Exploiting ultra-short α,β-peptides in the colloidal stabilization of gold nanoparticles

Raffaella Bucci[1]*, Daniela Maggioni[2], Silvia Locarno[3], Anna Maria Ferretti[4], Maria Luisa Gelmi[1] and Sara Pellegrino[1]*

[1] DISFARM-Dipartimento di Scienze Farmaceutiche, Sezione Chimica Generale e Organica ''A. Marchesini'', Università degli Studi di Milano, Via Venezian 21, 20133, Milano, Italy

[2] Dipartimento di Chimica, Università degli Studi di Milano, Via Golgi 19, 20133, Milano, Italy

[3] Dipartimento di Fisica "Aldo Pontremoli", Università degli Studi di Milano, Via Celoria 16, 20133 Milano (Italy)

[4] Istituto di Scienze e Tecnologie Chimiche "Giulio Natta", Consiglio Nazionale Delle Ricerche (SCITEC-CNR), Via G. Fantoli 16/15, Milano, 20138, Italy

raffaella.bucci@unimi.it

sara.pellegrino@unimi.it

Keyword

Gold Nanoparticles, Peptidomimetics, Dynamic Light Scattering, Protein Corona, Albumin Corona, Transmission electron microscopy, Hybrid Materials, Functionalized Gold Nanoparticles

Abstract

Colloidal gold nanoparticles (GNPs) have found wide-ranging applications in nanomedicine due to their unique optical properties, ease of preparation and functionalization. To avoid the formation of GNPs aggregates in the physiological environment, molecules such as lipids, polysaccharides or polymers are employed as GNPs coating. Here we present the colloidal stabilization of GNPs using ultra-short α,β-peptides containing the repeating unit of a diaryl $\beta^{2,3}$-amino acid and characterized by an extended conformation. Differently functionalized GNPs have been characterized by UV, DLS and TEM analysis, allowing defining the best candidate able to inhibit the aggregation of GNPs not only in water but also in mouse serum. In particular, a short tripeptide was found able to stabilize GNPs physiological media over three months. This new system has been further capped with albumin obtaining an even more colloidal stable material, able to prevent the formation of a thick protein corona in physiological medium.

Introduction

In recent years, nanotechnology is gaining a wide interest as a promising solution for the diverse impasses of science and nanomaterial-based technology is particularly exploited in biomedical applications, as imaging, biosensing, diagnostics and drug delivery. A recent trend has been dealing with the investigation of nanomaterials interactions with biological systems, known as nano-bio interactions. [1,2]

Among all the developed nanosystems for pharmaceutical applications, inorganic nanoparticles, as gold nanoparticles GNPs, represent one of the most appealing nanomaterials. In particular, GNPs, being easy to synthetize and engineer by varying size and surface composition,[3,4] have found wide-ranging applications in nanomedicine, including photothermal therapy, [5,6] drug delivery[7] and vaccine development.[8] Moreover, since the very beginning,[9] GNPs have proven to be powerful and versatile tools[10,11] also as a valid alternative to platinum-based anticancer coordination compounds for targeted cancer therapy.[12]

Unfortunately, only few examples of GNPs have progressed from the bench to the clinic. One successful case is CYT-6091, *i.e.* GNPs functionalized with PEG and recombinant human tumor necrosis factor-alpha showing positive outcomes for cancer therapy and are currently on clinical trials. [11] The main disadvantage of GNPs relies on their colloidal instability in the physiological environment, rich in proteins and salts that promote their aggregation. It is indeed known from the literature that GNPs can promote the formation of protein fibrils, inducing modifications in protein structures and leading to the growth of extended assemblies. [13,14] Moreover, once the particles are internalized, the proteins contained in the physiological medium form a coating called 'corona'. This protein layer is complex and could be very thick, often changing the GNPs properties, affecting thus the internalization process and the overall distribution in the body.[14]

To overcome these detrimental issues, stabilizing agents are commonly used, such as citrate and cetyltrimethylammonium bromide, although they are somehow unstable in several buffers.[15]

Another approach is the coating of GNPs with macromolecules such as lipids, polysaccharides, and polymers. In this contest, peptides appear particularly appealing for their unique features, such as biocompatibility, biodegradability,[16] ease in synthesis and chemical versatility.[16,17] Those Peptides can be designed to form self-assembled monolayers on gold nanoparticles to give nanomaterials with some chemical properties analogous to those of proteins. A variety of molecular-recognition properties are readily integrated within the peptide monolayer.[18] In addition, the possibility to introduce non-natural amino acid (AAs) in the sequence could give new functionalities or chemical features to the system[19–22] and increase both the metabolic [23,24] and conformational stability.[25–28] The possibility to modulate the secondary structure could be also particularly useful. On the other hand, while there is a widespread use of helical peptides for the stabilization of GNPs [29–32] only few examples of peptides with other conformations are present in literature,[10,33,34] and hence worth of new investigation.

Recently, we reported on the synthesis and characterization of different length α,β−peptides, containing repeating unit of dipeptide **D1** (Figure 1), composed by a (*R,R*)-diaryl $\beta^{2,3}$-AA and *L*-Ala. We observed that the $\beta^{2,3}$-AA can induce an extended conformation in solution, stabilizing the formation of a β-sheet structure through π,π−stacking. [35,36]

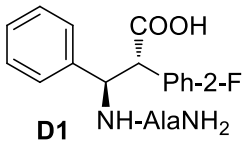

1: Ac-**D1**-Cys-$CONH_2$ **(MW:475.2; 65% yield)**
2: Ac-**D1**-**D1**-Cys-$CONH_2$ **(MW:786.3; 42% yield)**
3: Ac-**D1**-**D1**-**D1**-Cys-$CONH_2$ **(MW:1098.4; 37% yield)**

Figure 1: Chemical Formula of D1 and D1 peptide sequences with relative yields

Being intrigued by the use of peptides with extended conformation in solution as potential tools for the colloidal stabilization of GNPs, here we report on the synthesis and characterization of GNPs functionalized with peptides containing **D1** repeats and a cysteine at *C*- terminus, (compounds **1**, **2** and **3** in Figure 1). The introduction of the Cys- residue was indeed necessary for the decoration of the GNPs through a sulfur-gold bond. [37,38]

Using TEM, we showed that both peptides **1** and **2** are able to interact with the GNPs surface, while by both DLS and TEM experiments we proved that **1** and **2** inhibit the GNPs aggregation in water. Furthermore, experiments carried out on compound **1,** in the presence of either albumin or serum, pointed out the positive effect of the peptide coating in the prevention of aggregation under physiological conditions.

Result and Discussion

Synthesis

In view of preparing compounds **1-3** by solid phase peptide synthesis (SPPS), **Fmoc-D1** building block was synthesized in gram scale starting from the known **Boc-D1,** [39] as depicted in Scheme 1.

First, **Boc-D1** was deprotected both at of *C*- and *N*-termini with 1M HCl_{aq} affording intermediate **D1**. After protection at *N*-terminus with Fluorenylmethyloxycarbonyl- (Fmoc) group, **Fmoc-D1** was isolated in good yield.

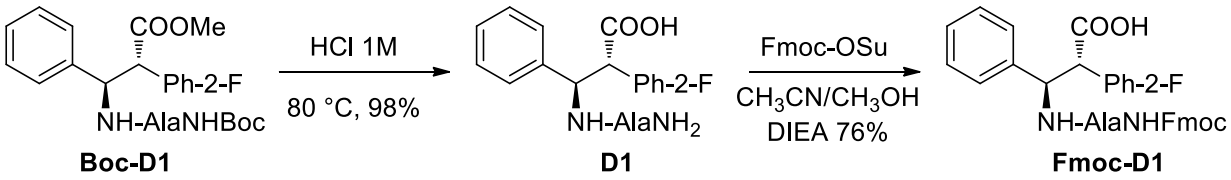

Scheme 1: Synthetic pathway for the preparation of Fmoc-D1

Peptides **1-3** were synthesized by Fmoc-based SPPS, using Rink amide resin (250 mg, 0.69 loading). After the Cys-loading, the *N*-Fmoc deprotection was performed using 20% Piperidine in DMF. Despite **Fmoc-D1** is a quite

hindered β-amino acid, its coupling was found efficient under the classical SPPS conditions. **Fmoc-D1** (5 eq.) was indeed coupled using HOBT/HBTU (5 eq.) as activators and DIEA (10 eq.) as the base. As highlighted in Figure 1, the overall peptide yields were quite satisfying. The secondary structure propensity of compounds **1**-**3** was investigated by FT-IR (see Supporting information, Figures S1-S3). In all cases, the predominance of extended conformation was observed, confirming the previous observation on Cys-free peptides.

Citrate coated GNPs were synthesized using Turkevich-Frens method, allowing the formation of monodispersed particles with 20 nm diameter [40,41]. GNPs functionalization with peptides was carried out following the ligand exchange procedure reported by Levy et al.[42] In order to find the right concentration of peptide for the nanoparticles functionalization, different volumes of a stock solution of 0.5 mM of the desired peptide were added to 2 mL of 0.9 nM GNPs, obtaining thus different peptide concentrations (**a**: $2.9 \cdot 10^{-3}$, **b**: $5.9 \cdot 10^{-3}$, **c**: $1.17 \cdot 10^{-2}$, **d**: $1.45 \cdot 10^{-2}$ mM). The GNPs were left under stirring overnight, allowing the ligand exchange reaction to keep on. UV-vis spectroscopy and Dynamic Light Scattering (DLS) analysis of functionalized GNPs in water were then carried out to find the best peptide ligand for further analyses in the physiological medium. Notice that, from now on, after the *at* symbol, we will indicate not only the number of the capping peptide, but when necessary, also the letter indicating the peptide concentration used in the ligand exchange step.

Functionalized GNPs: Characterization in water

Macroscopic differences between **1**, **2** and **3**-coated GNPs were already visible by the naked eye (Figure 2). Regarding GNP@**1**, all the samples appeared without any sign of aggregation (GNP@**1** in Figure 2). On the other hand, for GNP@**2**, the color of the last two samples slightly turned from red to purple, indicating that a possible aggregation phenomenon was occurring (GNP@**2c** and GNP@**2d** in Figure 2). Differently, in the case of the heptapeptide capped GNP@**3**, an immediate destabilization of the system was detected for all the concentration values, and even for the smallest amount of peptide used (GNP@**3a**), we observed incipient aggregation with brown aggregates detectable (GNP@**3** in Figure 2).

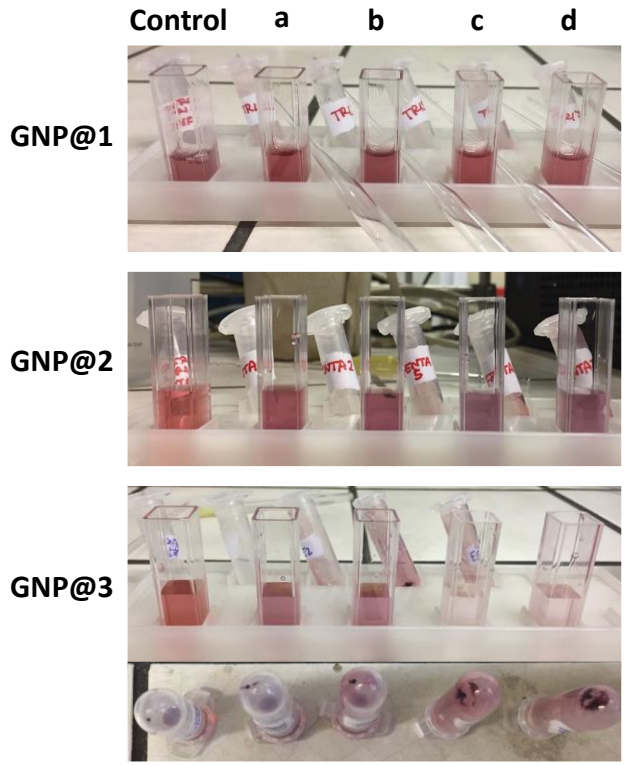

*Figure 2: Digital pictures of Peptide-Functionalized GNPs. From top to bottom: GNP@**1**, GNP@**2** and GNP@**3** water suspensions, with a particular focus on the brown aggregates present in GNP@**3** in the last row picture; from left to right citrate-GNPs (control), and citrate-GNPs after treatment with different amounts (**a**: $2.9 \cdot 10^{-3}$, **b**: $5.9 \cdot 10^{-3}$, **c**: $1.17 \cdot 10^{-2}$, **d**: $1.45 \cdot 10^{-2}$ mM) of the three peptides.*

GNP@**1a-d** and GNP@**2a-d** samples were thus characterized by UV-vis spectrosocopy, DLS analysis and TEM microscopy. UV-vis analyses were performed to get a confirmation of the possible ligand exchange between citrate and peptides **1** or **2**. It is indeed known that the absorption spectrum is sensitive to the nanoparticle environment and, when a ligand binds the GNPs, the change of the dielectric constant of the surrounding medium results in a slight change of the Surface Plasmon Resonance (SPR).[42] On the other hand, the destabilization of the system, due to the aggregate formation, caused an SPR band red-shift, which broadened significantly while reducing the peak extinction.[43,44]

In all cases (GNP@**1** and GNP@**2** at the different peptide concentrations), a slight shift of the SPR from 520 nm to 523-4 nm was detected, suggesting the occurrence of the ligand exchange (Figure 3). This shift demonstrated that the tripeptide **1** and pentapeptide **2** definitely interacted with the GNPs, replacing the citrate. As shown in Figure 3A, in the case of GNP@**1**, nanoparticles were always more stable –in terms of inhibition of aggregation- compared to the control, independently from the amount of peptide added, as shown by the higher SPR band intensity (Figure 3A). On the other hand, in case of GNP@**2**, GNP@**2c** and GNP@**2d**, appeared less stable being the SPR band much more reduced in intensity, largely red-shifted and asymmetrically enlarged by a shoulder, which is a clear indication of the beginning of an aggregation phenomenon.

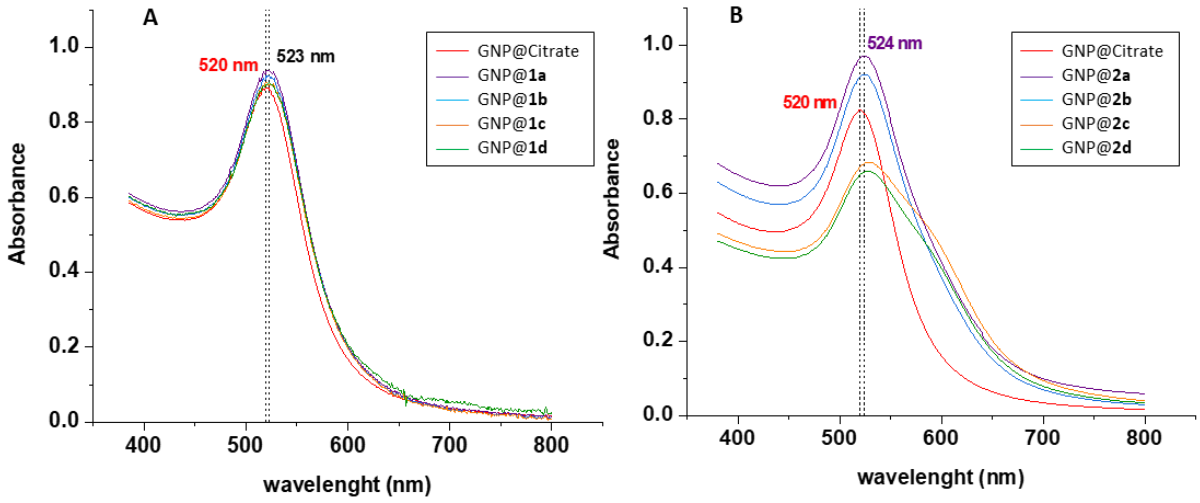

*Figure 3: UV-vis absorption Spectra of (A) **1**-GNP@**1** and (B) **2**-GNP@**2** in water. (**a**: 2.9·10^{-3}, **b**: 5.9·10^{-3}, **c**: 1.17·10^{-2}, **d**: 1.45·10^{-2} mM of added peptide)*

In Figure 4, DLS experiments on the most promising compounds are reported. The control GNP@citrate appeared monodispersed with an average hydrodynamic diameter of 25 nm. Being **1** and **2** very short peptides, in principle, no change in the hydrodynamic diameter of GNP@**1** and GNP@**2** was expected (Figure 3). In the case of GNP@**1**, the coated GNPs showed the same size than the GNP@citrate. Furthermore, we did not observe any aggregation peak apart of GNP@**1a** (Figure 3A). Concerning GNP@**2**, the hydrodynamic diameter increased from 25 nm to ca 80-90 nm (Figure 4B). DLS experiments were repeated periodically within three months, showing a very good colloidal stability of peptide-coated GNPs in comparison with GNP@citrate.

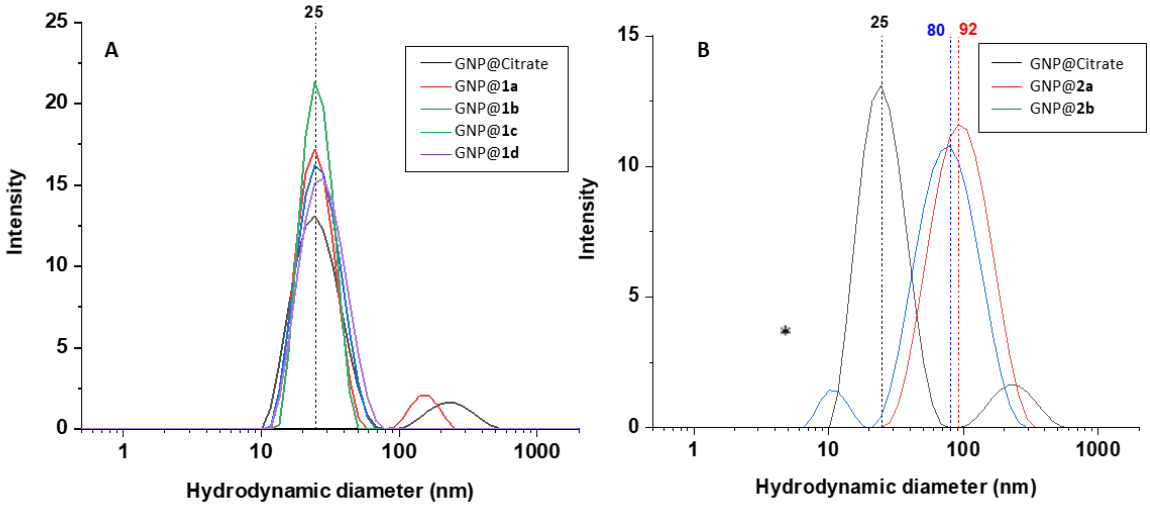

*Figure 4: Hydrodynamic diameter by DLS of GNP@**1** and GNP@**2** (being **a, b,c** and **d**: 2.9·10^{-3}, 5.9·10^{-3}, 1.17·10^{-2} and 1.45·10^{-2} mM concentrations of peptide **1** and **2**, respectively). The asterisk marks a small population of unlinked peptide aggregates.*

Functionalized GNPs: colloidal stability in Mouse serum.

Colloidal stability of the peptide capped GNPs was then evaluated in physiological environment. GNP@**1** and GNP@**2** were re-suspended in 10% mouse serum (whose DLS profile is reported in Figure S4), then the samples were left shaking for 24 hours and finally the medium discarded and changed with water, following the procedure reported in literature.[45,46]

From UV-vis spectroscopy analysis, GNP@**1** and GNP@**2** were found to be more colloidal stable than citrate-GNPs in 10% serum, as shown by the decreased intensity of the SPR band (Figure 5). Anyway, in the case of GNP@**2a** and GNP@**2b**, the asymmetric shape of the absorption band could indicate a possible beginning of aggregation phenomena.

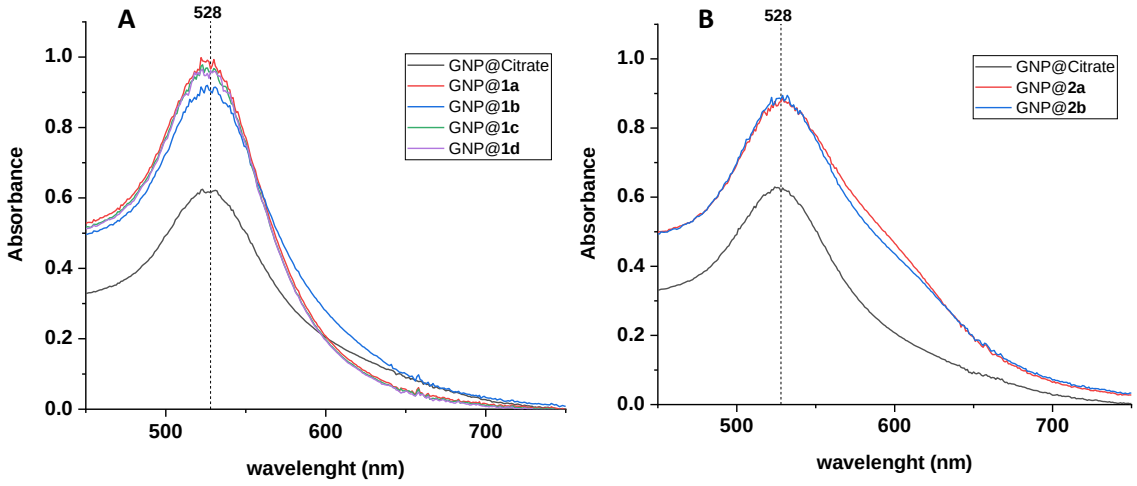

*Figure 5: UV-vis Spectra of GNP@**1** (A) and GNP@**2** (B) in Serum (aqueous solution 10%). **a, b,c** and **d**: $2.9 \cdot 10^{-3}$, $5.9 \cdot 10^{-3}$, $1.17 \cdot 10^{-2}$ and $1.45 \cdot 10^{-2}$ mM concentrations of peptide **1** and **2**, respectively.*

In the DLS experiments different populations were observed, indicating a possible interaction between the serum protein and the GNP@**1** and GNP@**2** (Figure S5 and S6 in SI). Among all, GNP@**1b** showed a DLS profile composed by two distinct peaks centered at 33 nm and 180 nm (Figure 6).

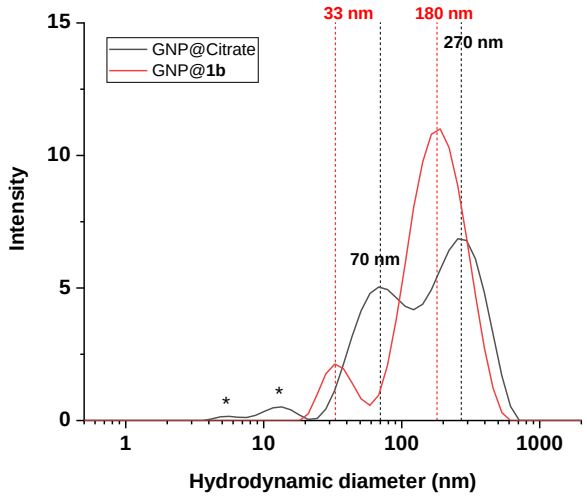

*Figure 6: Hydrodynamic diameter by DLS of GNP@**1b** after 10% serum incubation. **b**: 5.9·10^{-3} mM of added peptide **1**. The asterisks mark small amount of aggregated serum proteins*

In order to gain a further colloidal stabilization of GNPs in physiological conditions, we pretreated GNP@**1b** with albumin. Albumin is one of the main proteins contained in serum and works as cargo for small molecules such as metal ions, free fatty acids, hormones or drugs. It is known that pre-binding nanoparticles with albumin can increase the colloidal stability.[47,48] As a consequence, albumin is emerging as a versatile drug carrier in different applications in cancer therapy, due to its long-life and tendency to accumulate in tumors.[49] An example of this technology is the FDA approved drug Abraxane, a paclitaxel nanoparticle coated with albumin. It has been shown that the targeting of tumors enhances tumor penetration and minimizes toxicity compared to other forms of paclitaxel.[50] Albumin can interact easily with gold surface through electrostatic, hydrophobic interactions or chemisorption of the thiols to the gold surface.[51] Recently, 20 nm GNPs have been used as a model for understanding nanoparticle–HAS interactions highlighting that HAS is able to link gold surface via Cys53–Cys62 disulfide bond located at its subdomain IA.[52] Furthermore, it was found that BSA binding constant with GNPs is 7.59× 108 L/mol.[53]

GNP@**1b**, i.e. the best candidate among peptide-coated GNPs, was thus pre-treated with albumin and the obtained nano-system was studied by DLS and TEM microscopy experiments. First, GNP@**1b** were incubated with albumin for 2 days, favoring the formation of an albumin corona (Figure S7 in SI). In mouse serum, no sign of aggregation for GNP@**1b**@Albumin was detected neither by naked eye nor by DLS measurements. The DLS profile of GNP@**1b**@Albumin showed the presence of a GNP monodispersed population, i.e. one peak only centered at 110 nm (Figure 7), which is significantly smaller than for GNP@**1b** in serum (180 nm, Figure 6).

GNP@**1b**@Albumin showed a very high stability over three months in serum, while the control GNP@citrate in the same conditions started to aggregate after two days only.

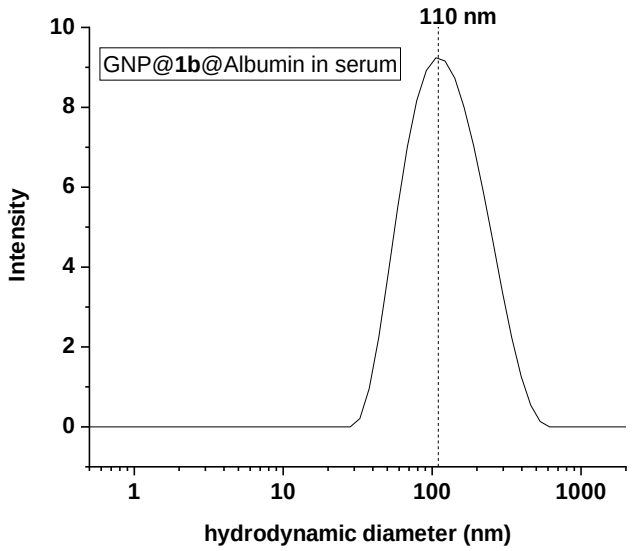

*Figure 7: DLS of Albumin-pretreated GNP@**1b** incubated with 10% serum, recovered by centrifugation, and re-suspended in water. b: $5.9 \cdot 10^{-3}$ mM of added peptide 1.*

For the sake of completeness, we studied also the stability of GNP@1b treated with albumin in physiological solution and compared with the starting GNP@citrate treated with albumin as well. The DLS data (see Figure S8) clearly show the higher stability of GNP covered with peptide **1** compared to GNP@citrate@albumin, which immeditely after resuspension in physiological solution changed color from red to blue indicating heavy aggregation was occurring.

TEM Microscopy

Control GNPs@Albumin and GNP@**1b**@Albumin were analyzed by TEM (Figure 8). The albumin shell is visible in both Control GNP@Albumin and GNP@**1b**@Albumin (Figures 8a and 8e). Surprisingly, in GNP@citrate, the albumin-shell is irregular and thicker than GNP@**1b**. The shell thickness was estimated around 2 nm in the first case and 1.6 nm in the second one. The energy selected image (ESI) collected at 24eV energy (Figures 8b and 8f) confirmed the organic nature of the shell, in white around the black metallic GNPs. This contrast is due to the plasmonic electrons which are present in organic compounds.[54,55]

The nature of the shell was further confirmed by the elemental maps of the calcium, being known the very high affinity of this ion for albumin.[56] Comparing the two samples, the advantage of the peptide coating on the GNPs

is evident: peptide coating indeed induces a better and more regular adhesion of the Albumin to the GNPs. Moreover, the absence of large agglomerates of free albumin is observed for GNP@**1b**.

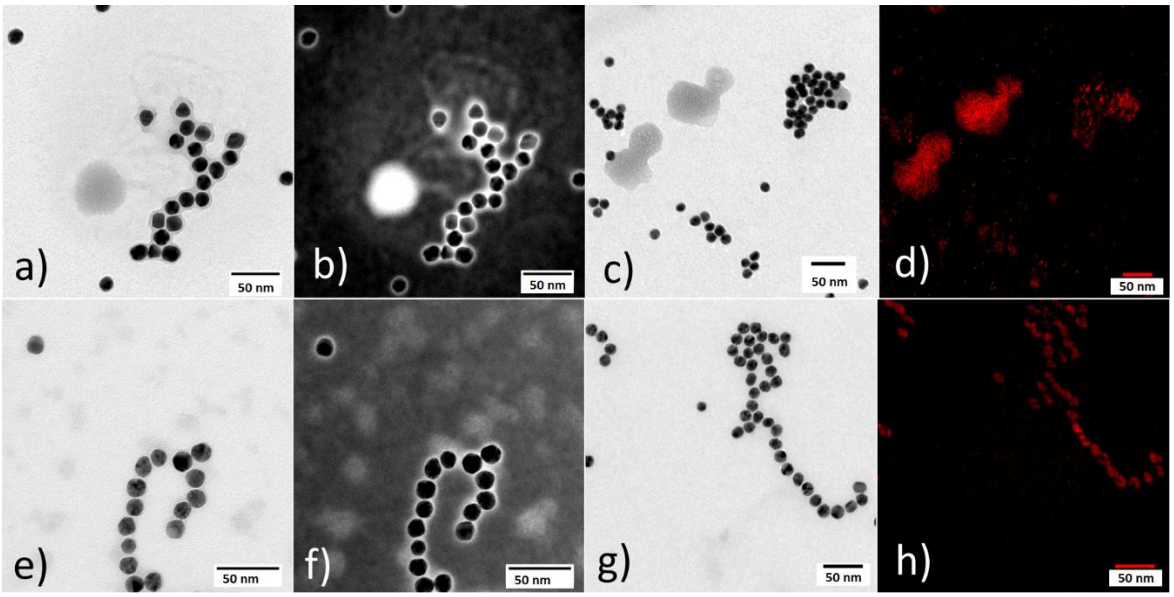

*Figure 8: GNP@citrate (a-d) and GNP@**1b** (e-h:) a, c, e, g are conventional TEM images, b and f are ESI images collected selecting 24eV of energy loss. d and h show the ion Ca elemental map. **b**: $5.9 \cdot 10^{-3}$ mM of added peptide **1**.*

In mouse serum, an interesting difference in control sample and GNP@**1b** was detected. Regarding control GNP@citrate (Figures 9a and 9b as ESI image), no evidence of an organic shell around the GNPs was present; on the contrary, some large organic agglomerates, indicating self-assembled serum proteins, were observed. On the other hand, an organic shell around albumin-pretreated GNP@**1b** was preserved (Figures 9d and 9e as ESI image; 1.5 nm thick). In this case, EELS analysis (Figures 9c and 9f) was carried out, demonstrating the calcium presence only in GNP@**1b** ($L_{2,3}$ signal of the calcium in the red square) and not in the control sample. This latter suggests that albumin is still bonded to the GNPs only in the case of a peptide **1**-coating. This is a further evidence that tripeptide **1** facilitates a stable interaction of albumin with the nanoparticle.

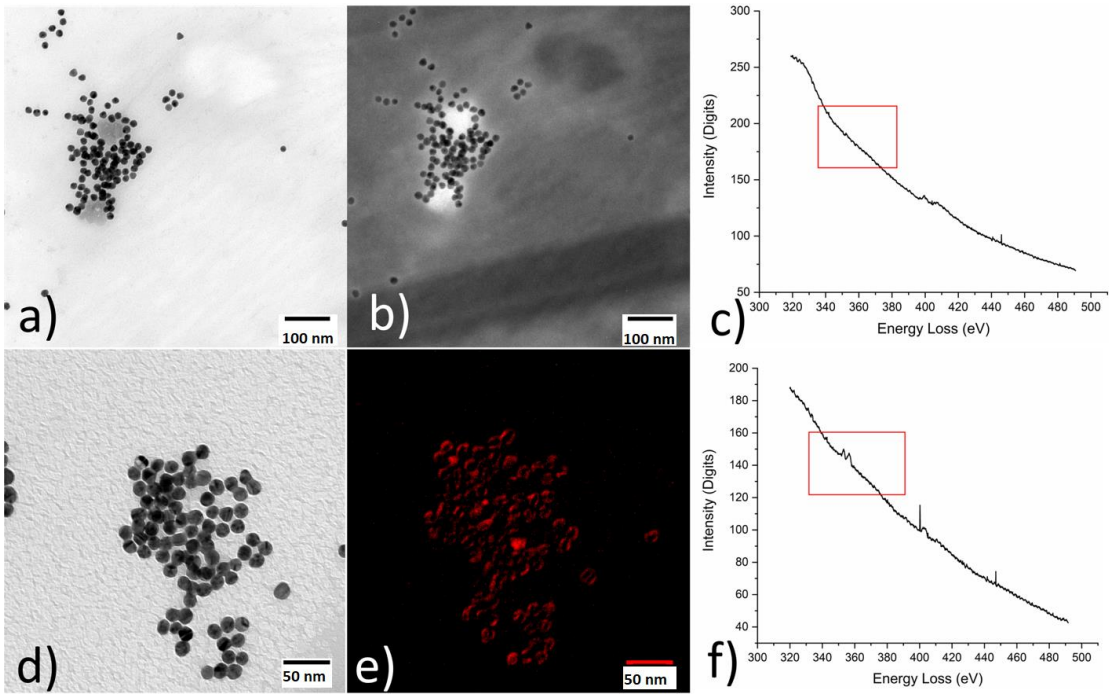

*Figure 9 (a): Conventional TEM images of Control GNPs in serum and (d): Albumin-Pretreated -GNP@**1b** in serum. (b): ESI image of Albumin-Pretreated Control GNPs in serum collected selecting 24eV of energy loss. (e): Calcium ESI map of the Albumin-Pretreated GNP@**1b**. (c and f): EELS spectra of the Control GNP@citrate and Albumin-Pretreated GNP@**1b** in serum respectively. The red square highlights the $L_{2,3}$, of the Calcium signal area. **b**: $5.9 \cdot 10^{-3}$ mM of added peptide **1**.*

Materials and Methods

Experimental Section

Experimental procedures, characterization data for newly synthesized compounds (^{1}H, ^{13}C NMR spectra for **Fmoc-D1** and **1**, Analitical HPLC and HRMS for Peptides **1**, **2** and **3**) are reported in the Supplementary Material.

Chemicals, Bovine Albumin and Mice Serum were purchased from Sigma Aldrich and Fluorochem and were used without further purification. ESI MS were recorded on a LCQ Advantage spectrometer from Thermo Finningan and a LCQ Fleet spectrometer from Thermo Scientific. Spectrograde $CDCl_3$ (99.8% D) was purchased from Fluka. The NMR spectroscopic experiments were carried out either on Varian MERCURY 300 MHz (300, 75 MHz for ^{1}H and ^{13}C respectively). Chemical shifts (δ) are given in ppm relative to the $CHCl_3$ internal standard, and the coupling constants *J* are reported in Hertz (Hz).

The Dynamic Light Scattering (DLS) measurements were performed using a Malvern Zetasizer Nano instrument at 25° C, equipped with a 633 nm solid state He–Ne laser at a scattering angle of 173°. Analyses were carried out in water (viscosity: 0.8872 Cp, refractive index: 1.33). The size measurements were averaged from at least three

repeated measurements. UV−vis absorption spectra were acquired on an Agilent model 8543 spectrophotometer at room temperature and using standard quartz cells with 1.0 cm path length.

The TEM images, electron energy loss spectroscopy (EELS), and electron spectroscopic imaging (ESI) of the gold nanoparticles (NPG) samples were performed by a Zeiss LIBRA 200FE-HR TEM, operating at 200 kV and equipped with a second generation in-column Ω filter for energy filtered imaging and diffraction. The EELS spectra were collected exciting a sample area of about 8 μm2. Elemental maps of Calcium were obtained by ESI at the corresponding $L_{2,3}$ edge using an energy window of 12 eV illumination angle 160 μrad, collection angle ∼13 mrad. The ESI images that highlight the presence of an organic shell around the gold nanoparticles were collected at 24eV. The Images were processed by means of the iTEM TEM Imaging Platform software (Olympus). The samples were prepared dropping 7 μL of gold nanoparticle suspension on a copper grid, let it dry overnight.

The size and the estimation of the gold nanoparticle size were performed using PEBBLES AND PEBBLE JUGGLER a software free to download.[57]

Peptide Synthesis

Peptides were synthesized using manual solid phase peptide synthesis on Rink amide resin using Fmoc protected amino acids and standard protocols[58]. Firstly, the *N*-Fmoc-protected amino acid was loaded on the resin. After *N*-deprotection with piperidine (20% in DMF), the following *N*-Fmoc-protected amino acid (5 eq.) was coupled to the resin using HOBT/HBTU (5 eq.) as activators and DIPEA (10 eq.) as the base. The Fmoc *N*-protecting group was removed, and the resin washed with DMF and DCM. Peptides were cleaved with a cleavage cocktail made of TFA (8 mL), water (200 μL), triisopropylsilane (400 μL), thioanisole (400 μL). The cleaved peptide was precipitated in cold diethylether and purified using the following RP-HPLC method: gradient elution of 5–95% solvent B (solvent A: water/acetonitrile/TFA, 95/5/0.1; solvent B: water/acetonitrile/TFA, 5/95/0.1) over 28 min at a flowrate of 20 mL/min using a C_{18} column.

GNPs Synthesis

$HAuCl_4 3H_2O$ (15 mg, 40 μmol) was dissolved in 150 mL of Milli-Q water and the solution was heated up to 100 °C. At this point a warm aqueous solution of trisodium citrate (70 °C) was poured in one portion and the system was refluxed for 60 minutes. The resulted nanoparticle suspension was then allowed to cool to r.t. stirring overnight.

According to the Mie theory[59] the GNPs size is correlated to the adsorbance at the Surface Plasma Resonance peak (λ_{max}). With a λ_{max} at 518 nm (see SI), the size average of GNPs is about 20 nm,[60] value that was confirmed

by DLS and TEM microscopy (see SI). From the Lambert Beer Law, the concentration of the GNPs batch was found to be around 0.9 nM, being the molar extinction coefficient (ε_{450}) 5.41E+08 $Lmol^{-1}cm^{-1}$.[61]

GNP Peptide-Coating

Different volumes of a stock solution of 0.5 mM of the desired peptide in DMSO were added to 2 mL of 0.9 nM GNP@citrate. The GNP@citrate were left under stirring overnight, allowing the ligand exchange reaction. In order to eliminate the citrate and the excess of peptides, the samples were washed with water after centrifugation at 20817 rcf for 15 minutes.

For the Albumin and Serum incubation, the GNPs were centrifuged and suspended in 10% Albumin or Serum in water. For DLS experiment the samples were then subject to another centrifugation and resuspension in water to avoid the presence of proteins aggregates.

Conclusion

In conclusion, we investigated about the possibility of using ultra-short extended peptides as colloidal stabilizers for GNPs, preventing their aggregation in physiological media. Our results demonstrated that the shortest tripeptide **1** is a promising candidate in the stabilization of GNPs. It was found that the pre-treatment of GNP@**1b** with albumin, prevents the formation of a thick protein corona and preserved GNPs colloidal stability in physiological media over three months. Thus, this work lays the foundation for this new hybrid system as a new candidate for nanomedicine applications, in particular in the development of stable, stealth GNPs.

Author Contribution S.P conceived the research. R. B. and S. L. prepared the Gold Nanoparticles. R.B. synthesized the peptides and functionalized the GNPs. R.B. and D.M. performed DLS and UV-vis experiments and interpreted the experimental data. A.F. performed TEM Experiments. R.B. and S.P. wrote the manuscript. M.L.G revised the text. All the authors reviewed the manuscript. The manuscript was written through contributions of all authors.

Conflicts of Interest The authors declare no conflict of interests.

Supporting Information

The Supporting Information is available free of charge at *link*. In the Table of contents: Synthesis of Fmoc-D1; Characterization of compounds 1,2,3; HRMS Spectra; NMR Spectra; FT-IR analyses on peptides 1,2 and 3; Stability

of functionalized GNP in mouse serum; Stability of functionalized GNP in NaCl 0.9%; UV and CD of compounds 1-3; TEM Experiments

References

(1) Roco, M. C. International Perspective on Government Nanotechnology Funding in 2005. *J. Nanoparticle Res.* **2005**, *7* (6), 707–712. https://doi.org/10.1007/s11051-005-3141-5.

(2) Albanese, A.; Tang, P. S.; Chan, W. C. W. The Effect of Nanoparticle Size, Shape, and Surface Chemistry on Biological Systems. *Annu. Rev. Biomed. Eng.* **2012**, *14* (1), 1–16. https://doi.org/10.1146/annurev-bioeng-071811-150124.

(3) Facchetti, G.; Rimoldi, I. Anticancer Platinum(II) Complexes Bearing N-Heterocycle Rings. *Bioorg. Med. Chem. Lett.* **2019**, *29* (11), 1257–1263. https://doi.org/https://doi.org/10.1016/j.bmcl.2019.03.045.

(4) Faraji, A. H.; Wipf, P. Nanoparticles in Cellular Drug Delivery. *Bioorg. Med. Chem.* **2009**, *17* (8), 2950–2962. https://doi.org/10.1016/J.BMC.2009.02.043.

(5) Daems, N.; Michiels, C.; Lucas, S.; Baatout, S.; Aerts, A. Gold Nanoparticles Meet Medical Radionuclides. *Nucl. Med. Biol.* **2021**, *100*, 61–90. https://doi.org/https://doi.org/10.1016/j.nucmedbio.2021.06.001.

(6) Riley, R. S.; Day, E. S. Gold Nanoparticle-Mediated Photothermal Therapy: Applications and Opportunities for Multimodal Cancer Treatment. *WIREs Nanomedicine and Nanobiotechnology* **2017**, *9* (4), e1449. https://doi.org/10.1002/wnan.1449.

(7) Dreaden, E. C.; Austin, L. A.; Mackey, M. A.; El-Sayed, M. A. Size Matters: Gold Nanoparticles in Targeted Cancer Drug Delivery. *Ther. Deliv.* **2012**, *3* (4), 457–478. https://doi.org/10.4155/tde.12.21.

(8) Almeida, J. P. M.; Lin, A. Y.; Figueroa, E. R.; Foster, A. E.; Drezek, R. A. In Vivo Gold Nanoparticle Delivery of Peptide Vaccine Induces Anti-Tumor Immune Response in Prophylactic and Therapeutic Tumor Models. *Small* **2015**, *11* (12), 1453–1459. https://doi.org/10.1002/smll.201402179.

(9) Thompson, D. Michael Faraday's Recognition of Ruby Gold: The Birth of Modern Nanotechnology. *Gold Bull.* **2007**, *40* (4), 267–269. https://doi.org/10.1007/BF03215598.

(10) Egorova, E. A.; van Rijt, M. M. J.; Sommerdijk, N.; Gooris, G. S.; Bouwstra, J. A.; Boyle, A. L.; Kros, A. One Peptide for Them All: Gold Nanoparticles of Different Sizes Are Stabilized by a Common Peptide Amphiphile. *ACS Nano* **2020**, *14* (5), 5874–5886. https://doi.org/10.1021/acsnano.0c01021.

(11) Chen, P. C.; Mwakwari, S. C.; Oyelere, A. K. Gold Nanoparticles: From Nanomedicine to Nanosensing. *Nanotechnol. Sci. Appl.* **2008**, *1*, 45–65. https://doi.org/10.2147/nsa.s3707.

(12) Medici, S.; Peana, M.; Coradduzza, D.; Zoroddu, M. A. Gold Nanoparticles and Cancer: Detection, Diagnosis and Therapy. *Semin. Cancer Biol.* **2021**. *Article in press* https://doi.org/https://doi.org/10.1016/j.semcancer.2021.06.017.

(13) Zhang, D.; Neumann, O.; Wang, H.; Yuwono, V. M.; Barhoumi, A.; Perham, M.; Hartgerink, J. D.; Wittung-Stafshede, P.; Halas, N. J. Gold Nanoparticles Can Induce the Formation of Protein-Based Aggregates at Physiological PH. *Nano Lett.* **2009**, *9* (2), 666–671. https://doi.org/10.1021/nl803054h.

(14) Singh, P.; Pandit, S.; Mokkapati, V. R. S. S.; Garg, A.; Ravikumar, V.; Mijakovic, I. Gold Nanoparticles in Diagnostics and Therapeutics for Human Cancer. *International Journal of Molecular Sciences*. 2018, p 1979. https://doi.org/10.3390/ijms19071979.

(15) Wang, A.; Ng, H. P.; Xu, Y.; Li, Y.; Zheng, Y.; Yu, J.; Han, F.; Peng, F.; Fu, L. Gold Nanoparticles: Synthesis, Stability Test, and Application for the Rice Growth. *J. Nanomater.* **2014**, *2014*, 451232. https://doi.org/10.1155/2014/451232.

(16) Ding, Y.; Sun, Z.; Tong, Z.; Zhang, S.; Min, J.; Xu, Q.; Zhou, L.; Mao, Z.; Xia, H.; Wang, W. Tumor Microenvironment-Responsive Multifunctional Peptide Coated Ultrasmall Gold Nanoparticles and Their Application in Cancer Radiotherapy. *Theranostics* **2020**, *10* (12), 5195–5208. https://doi.org/10.7150/thno.45017.

(17) Pellegrino, S.; Bonetti, A.; Clerici, F.; Contini, A.; Moretto, A.; Soave, R.; Gelmi, M. L. 1 *H* -Azepine-2-Oxo-5-Amino-5-Carboxylic Acid: A 3 $_{10}$ Helix Inducer and an Effective Tool for Functionalized Gold Nanoparticles. *J. Org. Chem.* **2015**, *80* (11), 5507–5516. https://doi.org/10.1021/acs.joc.5b00396.

(18) Lévy, R. Peptide-Capped Gold Nanoparticles: Towards Artificial Proteins. *ChemBioChem* **2006**, *7* (8), 1141–1145. https://doi.org/https://doi.org/10.1002/cbic.200600129.

(19) Bucci, R.; Bossi, A.; Erba, E.; Vaghi, F.; Saha, A.; Yuran, S.; Maggioni, D.; Gelmi, M. L.; Reches, M.; Pellegrino, S. Nucleobase Morpholino β Amino Acids as Molecular Chimeras for the Preparation of Photoluminescent Materials from Ribonucleosides. *Sci. Rep.* **2020**, *10* (1), 19331. https://doi.org/10.1038/s41598-020-76297-7.

(20) Pellegrino, S.; Facchetti, G.; Contini, A.; Gelmi, M. L.; Erba, E.; Gandolfi, R.; Rimoldi, I. Ctr-1 Mets7 Motif Inspiring New Peptide Ligands for Cu(i)-Catalyzed Asymmetric Henry Reactions under Green Conditions. *RSC Adv.* **2016**, *6* (75), 71529–71533. https://doi.org/10.1039/c6ra16255j.

(21) Rimoldi, I.; Bucci, R.; Feni, L.; Santagostini, L.; Facchetti, G.; Pellegrino, S. Exploring the Copper Binding Ability of Mets7 HCtr-1 Protein Domain and His7 Derivative: An Insight in Michael Addition Catalysis. *J. Pept. Sci.* **2020**, *27* (e3289), 1–7. https://doi.org/10.1002/psc.3289.

(22) Bucci, R.; Foschi, F.; Loro, C.; Erba, E.; Gelmi, M. L.; Pellegrino, S. Fishing in the Toolbox of Cyclic Turn Mimics: A Literature Overview of the Last Decade. *European J. Org. Chem.* **2021**, *2021* (20), 2887–2900. https://doi.org/https://doi.org/10.1002/ejoc.202100244.

(23) Contini, A.; Ferri, N.; Bucci, R.; Lupo, M. G.; Erba, E.; Gelmi, M. L.; Pellegrino, S. Peptide Modulators of Rac1/Tiam1 Protein-Protein Interaction: An Alternative Approach for Cardiovascular Diseases. *Pept. Sci.* **2017**, *110* (e23089), 1–8. https://doi.org/10.1002/bip.23089.

(24) Heck, T.; Limbach, M.; Geueke, B.; Zacharias, M.; Gardiner, J.; Kohler, H.-P.; Seebach, D. Enzymatic Degradation of β- and Mixed α,β-Oligopeptides. *Chem. Biodivers.* **2006**, *3*, 1325.

(25) Vaghi, F.; Bucci, R.; Clerici, F.; Contini, A.; Gelmi, M. L. Non-Natural 3-Arylmorpholino-β-Amino Acid as a PPII Helix Inducer. *Org. Lett.* **2020**, *22* (15), 6197–6202. https://doi.org/10.1021/acs.orglett.0c02331.

(26) Oliva, F.; Bucci, R.; Tamborini, L.; Pieraccini, S.; Pinto, A.; Pellegrino, S. Bicyclic Pyrrolidine-Isoxazoline γ Amino Acid: A Constrained Scaffold for Stabilizing α-Turn Conformation in Isolated Peptides. *Front. Chem.* **2019**, *7* (March), 1–10. https://doi.org/10.3389/fchem.2019.00133.

(27) Bucci, R.; Contini, A.; Clerici, F.; Pellegrino, S.; Gelmi, M. L. From Glucose to Enantiopure Morpholino β-Amino Acid: A New Tool for Stabilizing γ-Turns in Peptides. *Org. Chem. Front.* **2019**, *6*, 972–982. https://doi.org/10.1039/C8QO01116H.

(28) Bucci, R.; Giofré, S.; Clerici, F.; Contini, A.; Pinto, A.; Erba, E.; Soave, R.; Pellegrino, S.; Gelmi, M. L. Tetrahydro-4 H-(Pyrrolo[3,4- d]Isoxazol-3-Yl)Methanamine: A Bicyclic Diamino Scaffold Stabilizing Parallel Turn Conformations. *J. Org. Chem.* **2018**, *83* (19), 11493–11501.

https://doi.org/10.1021/acs.joc.8b01299.

(29) Higashi, N.; Kawahara, J.; Niwa, M. Preparation of Helical Peptide Monolayer-Coated Gold Nanoparticles. *J. Colloid Interface Sci.* **2005**, *288* (1), 83–87. https://doi.org/https://doi.org/10.1016/j.jcis.2005.02.086.

(30) Pengo, P.; Broxterman, Q. B.; Kaptein, B.; Pasquato, L.; Scrimin, P. Synthesis of a Stable Helical Peptide and Grafting on Gold Nanoparticles. *Langmuir* **2003**, *19* (6), 2521–2524. https://doi.org/10.1021/la025982v.

(31) Wilder, L. M.; Fies, W. A.; Rabin, C.; Webb, L. J.; Crooks, R. M. Conjugation of an α-Helical Peptide to the Surface of Gold Nanoparticles. *Langmuir* **2019**, *35* (9), 3363–3371. https://doi.org/10.1021/acs.langmuir.9b00075.

(32) Longo, E.; Orlandin, A.; Mancin, F.; Scrimin, P.; Moretto, A. Reversible Chirality Control in Peptide-Functionalized Gold Nanoparticles. *ACS Nano* **2013**, *7* (11), 9933–9939. https://doi.org/10.1021/nn403816a.

(33) Tkachenko, A. G.; Xie, H.; Coleman, D.; Glomm, W.; Ryan, J.; Anderson, M. F.; Franzen, S.; Feldheim, D. L. Multifunctional Gold Nanoparticle−Peptide Complexes for Nuclear Targeting. *J. Am. Chem. Soc.* **2003**, *125* (16), 4700–4701. https://doi.org/10.1021/ja0296935.

(34) Shaw, C. P.; Middleton, D. A.; Volk, M.; Lévy, R. Amyloid-Derived Peptide Forms Self-Assembled Monolayers on Gold Nanoparticle with a Curvature-Dependent β-Sheet Structure. *ACS Nano* **2012**, *6* (2), 1416–1426. https://doi.org/10.1021/nn204214x.

(35) Bucci, R.; Contini, A.; Clerici, F.; Beccalli, E. M.; Formaggio, F.; Maffucci, I.; Pellegrino, S.; Gelmi, M. L. Fluoro-Aryl Substituted α,β 2,3 -Peptides in the Development of Foldameric Antiparallel β-Sheets: A Conformational Study. *Front. Chem.* **2019**, *7* (APR), 1–11. https://doi.org/10.3389/fchem.2019.00192.

(36) Bonetti, A.; Pellegrino, S.; Das, P.; Yuran, S.; Bucci, R.; Ferri, N.; Meneghetti, F.; Castellano, C.; Reches, M.; Gelmi, M. L. Dipeptide Nanotubes Containing Unnatural Fluorine-Substituted Beta2,3-Diarylamino Acid and l-Alanine as Candidates for Biomedical Applications. *Org. Lett.* **2015**, *17* (18), 4468–4471. https://doi.org/10.1021/acs.orglett.5b02132.

(37) Crespo, P.; Litrán, R.; Rojas, T. C.; Multigner, M.; de la Fuente, J. M.; Sánchez-López, J. C.; García, M. A.; Hernando, A.; Penadés, S.; Fernández, A. Permanent Magnetism, Magnetic Anisotropy, and Hysteresis of Thiol-Capped Gold Nanoparticles. *Phys. Rev. Lett.* **2004**, *93* (8), 87204. https://doi.org/10.1103/PhysRevLett.93.087204.

(38) Li, Z.; Jin, R.; Mirkin, C. A.; Letsinger, R. L. Multiple Thiol-Anchor Capped DNA–Gold Nanoparticle Conjugates. *Nucleic Acids Res.* **2002**, *30* (7), 1558–1562. https://doi.org/10.1093/nar/30.7.1558.

(39) Bonetti, A.; Clerici, F.; Foschi, F.; Nava, D.; Pellegrino, S.; Penso, M.; Soave, R.; Gelmi, M. L. Syn / Anti Switching by Specific Heteroatom – Titanium Coordination in the Mannich-Like Synthesis of 2 , 3-Diaryl-β -Amino Acid Derivatives. *European J. Org. Chem.* **2014**, 3203–3209. https://doi.org/10.1002/ejoc.201400142.

(40) Turkevich, J.; Stevenson, P. C.; Hillier, J. A Study of the Nucleation and Growth Processes in the Synthesis of Colloidal Gold. *Discuss. Faraday Soc.* **1951**, *11* (0), 55–75. https://doi.org/10.1039/DF9511100055.

(41) Giljohann, D. A.; Seferos, D. S.; Daniel, W. L.; Massich, M. D.; Patel, P. C.; Mirkin, C. A. Gold Nanoparticles for Biology and Medicine. *Angew. Chemie Int. Ed.* **2010**, *49* (19), 3280–3294. https://doi.org/10.1002/anie.200904359.

(42) Lévy, R.; Thanh, N. T. K.; Doty, R. C.; Hussain, I.; Nichols, R. J.; Schiffrin, D. J.; Brust, M.; Fernig, D. G. Rational and Combinatorial Design of Peptide Capping Ligands for Gold Nanoparticles. *J. Am. Chem. Soc.* **2004**, *126* (32), 10076–10084. https://doi.org/10.1021/ja0487269.

(43) Storhoff, J. J.; Lazarides, A. A.; Mucic, R. C.; Mirkin, C. A.; Letsinger, R. L.; Schatz, G. C. What Controls the Optical Properties of DNA-Linked Gold Nanoparticle Assemblies? *J. Am. Chem. Soc.* **2000**, *122* (19), 4640–4650. https://doi.org/10.1021/ja993825l.

(44) Tullman, J. A.; Finney, W. F.; Lin, Y.-J.; Bishnoi, S. W. Tunable Assembly of Peptide-Coated Gold Nanoparticles. *Plasmonics* **2007**, *2* (3), 119–127. https://doi.org/10.1007/s11468-007-9033-z.

(45) Chuang, C.-C.; Chang, C.-W. Complexation of Bioreducible Cationic Polymers with Gold Nanoparticles for Improving Stability in Serum and Application on Nonviral Gene Delivery. *ACS Appl. Mater. Interfaces* **2015**, *7* (14), 7724–7731. https://doi.org/10.1021/acsami.5b00732.

(46) Pooja, D.; Panyaram, S.; Kulhari, H.; Rachamalla, S. S.; Sistla, R. Xanthan Gum Stabilized Gold Nanoparticles: Characterization, Biocompatibility, Stability and Cytotoxicity. *Carbohydr. Polym.* **2014**, *110*, 1–9. https://doi.org/https://doi.org/10.1016/j.carbpol.2014.03.041.

(47) Curnis, F.; Sacchi, A.; Longhi, R.; Colombo, B.; Gasparri, A.; Corti, A. IsoDGR-Tagged Albumin: A New Avβ3 Selective Carrier for Nanodrug Delivery to Tumors. *Small* **2013**, *9* (5), 673–678. https://doi.org/10.1002/smll.201202310.

(48) Yang, H.; Fung, S.-Y.; Liu, M. Programming the Cellular Uptake of Physiologically Stable Peptide-Gold Nanoparticle Hybrids with Single Amino Acids. *Angew. Chemie* **2011**, *123* (41), 9817–9820. https://doi.org/10.1002/ange.201102911.

(49) M, H.; Azzazy, E.; Christenson, R. H. All About Albumin: Biochemistry, Genetics, and Medical Applications. Theodore Peters, Jr. San Diego, CA: Academic Press, 1996, 432 Pp, $85.00. ISBN 0-12-552110-3. *Clin. Chem.* **1997**, *43* (10), 2014a – 2015. https://doi.org/10.1093/clinchem/43.10.2014a.

(50) Aggarwal, P.; Hall, J. B.; McLeland, C. B.; Dobrovolskaia, M. A.; McNeil, S. E. Nanoparticle Interaction with Plasma Proteins as It Relates to Particle Biodistribution, Biocompatibility and Therapeutic Efficacy. *Adv. Drug Deliv. Rev.* **2009**, *61* (6), 428–437. https://doi.org/https://doi.org/10.1016/j.addr.2009.03.009.

(51) Bolaños, K.; Kogan, M. J.; Araya, E. Capping Gold Nanoparticles with Albumin to Improve Their Biomedical Properties. *Int. J. Nanomedicine* **2019**, *14*, 6387–6406. https://doi.org/10.2147/IJN.S210992.

(52) Sen, T.; Mandal, S.; Haldar, S.; Chattopadhyay, K.; Patra, A. Interaction of Gold Nanoparticle with Human Serum Albumin (HSA) Protein Using Surface Energy Transfer. *J. Phys. Chem. C* **2011**, *115* (49), 24037–24044. https://doi.org/10.1021/jp207374g.

(53) Shi, X.; Li, D.; Xie, J.; Wang, S.; Wu, Z.; Chen, H. Spectroscopic Investigation of the Interactions between Gold Nanoparticles and Bovine Serum Albumin. *Chinese Sci. Bull.* **2012**, *57* (10), 1109–1115. https://doi.org/10.1007/s11434-011-4741-3.

(54) Galli, M.; Rossotti, B.; Arosio, P.; Ferretti, A. M.; Panigati, M.; Ranucci, E.; Ferruti, P.; Salvati, A.; Maggioni, D. A New Catechol-Functionalized Polyamidoamine as an Effective SPION Stabilizer. *Colloids Surfaces B Biointerfaces* **2019**, *174*, 260–269. https://doi.org/https://doi.org/10.1016/j.colsurfb.2018.11.007.

(55) Drummy, L. F.; Davis, R. J.; Moore, D. L.; Durstock, M.; Vaia, R. A.; Hsu, J. W. P. Molecular-Scale and Nanoscale Morphology of P3HT:PCBM Bulk Heterojunctions: Energy-Filtered TEM and Low-Dose HREM. *Chem. Mater.* **2011**, *23* (3), 907–912. https://doi.org/10.1021/cm102463t.

(56) Katz, S.; Klotz, I. M. Interactions of Calcium with Serum Albumin. *Arch. Biochem. Biophys.* **1953**, *44* (2), 351–361. https://doi.org/https://doi.org/10.1016/0003-9861(53)90054-X.

(57) Mondini, S.; Ferretti, A. M.; Puglisi, A.; Ponti, A. Pebbles and PebbleJuggler: Software for Accurate, Unbiased, and Fast Measurement and Analysis of Nanoparticle Morphology from Transmission Electron Microscopy (TEM) Micrographs. *Nanoscale* **2012**, *4* (17), 5356–5372. https://doi.org/10.1039/C2NR31276J.

(58) Pellegrino, S.; Annoni, C.; Contini, A.; Clerici, F.; Gelmi, M. L. Expedient Chemical Synthesis of 75mer DNA Binding Domain of MafA: An Insight on Its Binding to Insulin Enhancer. *Amino Acids* **2012**, *43* (5), 1995–2003. https://doi.org/10.1007/s00726-012-1274-2.

(59) Link, S.; El-Sayed, M. A. Shape and Size Dependence of Radiative, Non-Radiative and Photothermal Properties of Gold Nanocrystals. *Int. Rev. Phys. Chem.* **2000**, *19* (3), 409–453. https://doi.org/10.1080/01442350050034180.

(60) Njoki, P. N.; Lim, I.-I. S.; Mott, D.; Park, H.-Y.; Khan, B.; Mishra, S.; Sujakumar, R.; Luo, J.; Zhong, C.-J. Size Correlation of Optical and Spectroscopic Properties for Gold Nanoparticles. *J. Phys. Chem. C* **2007**, *111* (40), 14664–14669. https://doi.org/10.1021/jp074902z.

(61) Haiss, W.; Thanh, N. T. K.; Aveyard, J.; Fernig, D. G. Determination of Size and Concentration of Gold Nanoparticles from UV−Vis Spectra. *Anal. Chem.* **2007**, *79* (11), 4215–4221. https://doi.org/10.1021/ac0702084.

TOC Graphic

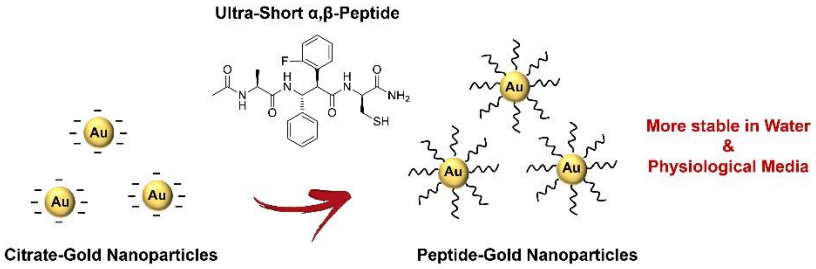
Ultra-Short α,β-Peptide
F
NH2
SH
Au
Au
Au
Au
Au
Au
More stable in Water
&
Physiological Media
Citrate-Gold Nanoparticles
Peptide-Gold Nanoparticles